Kinesin-5/Eg5 is important for transport of CARTS from the trans-Golgi network to the cell surface

Yuichi Wakana,[1,2,3] Julien Villeneuve,[1,2] Josse van Galen,[1,2] David Cruz-Garcia,[1,2] Mitsuo Tagaya,[3] and Vivek Malhotra[1,2,4]

[1]Cell and Developmental Biology Programme, Centre for Genomic Regulation (CRG), 08003 Barcelona, Spain
[2]Universitat Pompeu Fabra (UPF), 08003 Barcelona, Spain
[3]School of Life Sciences, Tokyo University of Pharmacy and Life Sciences, Hachioji, Tokyo 192-0392, Japan
[4]Institució Catalana de Recerca i Estudis Avançats (ICREA), 08010 Barcelona, Spain

Here we report that the kinesin-5 motor Klp61F, which is known for its role in bipolar spindle formation in mitosis, is required for protein transport from the Golgi complex to the cell surface in *Drosophila* S2 cells. Disrupting the function of its mammalian orthologue, Eg5, in HeLa cells inhibited secretion of a protein called pancreatic adenocarcinoma up-regulated factor (PAUF) but, surprisingly, not the trafficking of vesicular stomatitis virus G protein (VSV-G) to the cell surface.

We have previously reported that PAUF is transported from the trans-Golgi network (TGN) to the cell surface in specific carriers called CARTS that exclude VSV-G. Inhibition of Eg5 function did not affect the biogenesis of CARTS; however, their migration was delayed and they accumulated near the Golgi complex. Altogether, our findings reveal a surprising new role of Eg5 in nonmitotic cells in the facilitation of the transport of specific carriers, CARTS, from the TGN to the cell surface.

Introduction

The newly synthesized secretory proteins are first transported from the endoplasmic reticulum (ER) to the Golgi complex (Zanetti et al., 2012). At the Golgi complex, the cargo is sorted, based on specific signals, and then packed into respective carriers for delivery to their target compartments or for secretion from the cells (Mellman and Nelson, 2008; Anitei and Hoflack, 2011). The microtubule-associated motor protein kinesin family members play an important role in the efficient trafficking of the transport carriers from the TGN to the plasma membrane. The examples include kinesin-1 family members (KIF5A and KIF5B) and kinesin-3 (KIF13A) for the migration of carriers to the cell surface; KIF5B, KIF5C, and kinesin-14 (KIFC3) to the apical surface in polarized cells (Nakagawa et al., 2000; Noda et al., 2001; Vale, 2003; Grigoriev et al., 2007; Jaulin et al., 2007; Hirokawa and Noda, 2008; Astanina and Jacob, 2010; Burgo et al., 2012).

We have identified a specific class of transport carriers called CARTS (carriers of the TGN to the cell surface) that are produced at the TGN and contain proteins such as pancreatic adenocarcinoma up-regulated factor (PAUF), TGN46, and lysozyme C, but exclude vesicular stomatitis virus G protein (VSV-G) and collagen I (Wakana et al., 2012). We present our findings that the kinesin Eg5 is required for the migration of CARTS toward the cell surface in nonmitotic cells during protein secretion. Eg5, a kinesin-5 family member (Lawrence et al., 2004), is well known for its role in bipolar spindle assembly during mitosis (Le Guellec et al., 1991; Hagan and Yanagida, 1992; Saunders and Hoyt, 1992; Sawin et al., 1992; Heck et al., 1993; Cole et al., 1994; Blangy et al., 1995; Cottingham et al., 1999; Valentine et al., 2006). Eg5 is known to cross-link and slide anti-parallel microtubules and is thus crucial for the assembly of a bipolar spindle during mitosis (Sharp et al., 1999; Kapoor and Mitchison, 2001; Kwok et al., 2004; Miyamoto et al., 2004; Kapitein et al., 2005; Brust-Mascher et al., 2009). The requirement of Eg5 in the migration of CARTS is therefore quite surprising and suggests a new mechanism for its function in nonmitotic cells. The description of our data follows.

J. Villeneuve, J. van Galen, and D. Cruz-Garcia contributed equally to this paper.

Correspondence to Vivek Malhotra: Vivek.Malhotra@crg.eu; or Yuichi Wakana: ywakana@toyaku.ac.jp

Abbreviations used in this paper: CARTS, carriers of the trans-Golgi network to the cell surface; PAUF, pancreatic adenocarcinoma up-regulated factor; ssHRP, signal sequence horseradish peroxidase; VSV-G, vesicular stomatitis virus G protein.

THE JOURNAL OF CELL BIOLOGY

Results and discussion

Klp61F is required for the post-Golgi trafficking of secretory cargo

A genome-wide screen revealed that a kinesin-5 motor called Klp61F was required for protein secretion by *Drosophila* S2 cells (Bard et al., 2006). Given the established role of Klp61F and its orthologues in bipolar spindle assembly during mitosis, we reinvestigated this potentially new function of Klp61F in nonmitotic cells.

Drosophila S2 cells transformed to stably express signal sequence and V5-tagged horseradish peroxidase (ssHRP-V5) on an inducible promoter were transfected with double-stranded RNA (dsRNA) specific for Klp61F, TANGO1, twinstar, or LacZ (control). The knockdown efficiency was determined by RT-PCR, which revealed a strong reduction of the respective mRNA (Fig. 1 A). After 5 d of incubation with dsRNA, the cells were incubated with Cu^{2+} to initiate the synthesis of ssHRP-V5. 12 h later, the medium and the cell lysates were tested for HRP activity by enhanced chemiluminescence (ECL). We found that the activity of HRP in the medium of Klp61F knockdown cells was reduced, which is comparable to the effects of the knockdown of TANGO1 and twinstar (Fig. 1 B). We also Western blotted the medium with anti-V5 antibody to rule out the possibility that reduced HRP signal in the medium was due to effects on the activity, measured by ECL, and not the actual levels of HRP. The results revealed a decrease in the level of HRP secreted by Klp61F knockdown cells compared with control cells (Fig. 1 C). Western blotting the cell lysate of Klp61F knockdown cells revealed HRP as two distinct polypeptides of 50 and 65 kD, respectively (Fig. 1 D). HRP requires TANGO1 for its export from the ER (Saito et al., 2009). In TANGO1 knockdown cells, HRP was found as a 65-kD polypeptide. Twinstar knockdown arrests HRP in the TGN (von Blume et al., 2009) and upon knockdown of twinstar HRP is present as a polypeptide of 50 kD. The 65- and 50-kD polypeptides are therefore likely the ER and Golgi form of HRP, respectively. The presence of HRP in Klp61F knockdown cells as a polypeptide of 50 kD therefore suggests a defect in its trafficking from the Golgi complex to cell surface step of the secretory pathway (Fig. 1, D and E).

Eg5 is required at a post-Golgi step of the secretory pathway

To further ascertain the role of Klp61F in secretion, we tested the requirement of its mammalian orthologue, Eg5, in the secretion of a protein called PAUF. HeLa cells were transfected with siRNA oligos specific for Eg5 or a control oligo. Two siRNA oligos targeting a different sequence of Eg5, siRNA (207) and siRNA (608), reduced the expression of Eg5 by ∼70% compared with the control siRNA (Fig. 2, A and B). The siRNA-based knockdown of Eg5 was repeated, and 20 h after siRNA transfection HeLa cells were transfected with a plasmid encoding MycHis-tagged PAUF and incubated in the presence of 2 mM thymidine to prevent cells from entering mitosis. 20 h later, the cells were incubated at 20°C for 2 h to arrest secretory cargo at the TGN, washed with fresh medium, and then shifted to 32°C for 1 h to restart cargo export. In the absence of thymidine a monopolar spindle was observed in greater than 90% of mitotic cells, indicating that the function of Eg5 was significantly impaired upon Eg5 knockdown (Fig. 2 C). In thymidine-treated cells, knockdown of Eg5 had no obvious effect on the organization of cytoplasmic microtubules and the Golgi complex (Fig. 2 D and Fig. S1 A). There was also no effect on their reassembly after treatment with the microtubule-depolymerizing drug nocodazole (Fig. S1 B). The medium from Eg5 knockdown and control cells was Western blotted with anti-His antibody to determine secreted PAUF-MycHis. Interestingly, in the presence of thymidine (in nonmitotic cells), knockdown of Eg5 inhibited PAUF-MycHis secretion by ∼50% compared with control cells (Fig. 2, E and F).

We then tested the effect of a specific Eg5 inhibitor, monastrol (Mayer et al., 1999), on PAUF secretion. HeLa cells expressing PAUF-MycHis were incubated at 20°C for 2 h, treated with monastrol or dimethyl sulfoxide (DMSO) for 15 min, and then shifted to 32°C for 45 min to restart cargo export. Monastrol treatment inhibited PAUF-MycHis secretion by ∼65% compared with DMSO-treated cells (Fig. 3, A and B). We also tested the effect of monastrol treatment on HRP secretion. HeLa cells stably expressing ssHRP (HeLa-ssHRP cells) were incubated with fresh medium in the presence of monastrol or DMSO. At the indicated times, the medium was collected to measure HRP activity by ECL. Monastrol treatment severely affected the kinetics of HRP secretion (Fig. 3 C). In contrast to Eg5 knockdown, knockdown of kinesin-12 and kinesin-10 (KIF15 and KIF22, respectively) had no effect on the kinetics of HRP secretion (Fig. S2). Treatment with monastrol did not affect the organization of cytoplasmic microtubules or the Golgi complex in nonmitotic cells (Fig. S1 C).

PAUF and HRP are transported from the TGN in carriers called CARTS that exclude VSV-G (Wakana et al., 2012). We tested whether Eg5 was required for VSV-G transport from the TGN. HeLa cells stably expressing VSV-G fused with GFP (HeLa-VSV-G-GFP cells) were cultured at 40°C for 48 h to synchronize cargo export from the ER. The cells were incubated at 20°C in the presence of cycloheximide for 2 h and monastrol was added in the last 15 min of this incubation. The cells were then transferred to 32°C to restore cargo export from the TGN. Analysis by microscopy showed that monastrol treatment did not affect the trafficking of VSV-G-GFP (Fig. 3, D and E). This result was confirmed by a quantitative cell surface biotinylation assay (Fig. 3 F).

CARTS move on microtubules

HeLa cells expressing PAUF fused with monomeric red fluorescent protein (mRFP) were visualized by fluorescence microscopy with anti–α-tubulin antibody. PAUF-mRFP containing CARTS appeared as discrete punctate elements along the cytoplasmic microtubules (Fig. S3 A). Live-cell imaging showed that PAUF-containing CARTS migrate on microtubules (Video 1). Next, HeLa cells were cotransfected with plasmids for PAUF-MycHis and GFP-Eg5, fixed, and visualized by fluorescence microscopy with anti-Myc antibody. GFP-Eg5 was present throughout the cytoplasm (Fig. S3 B,
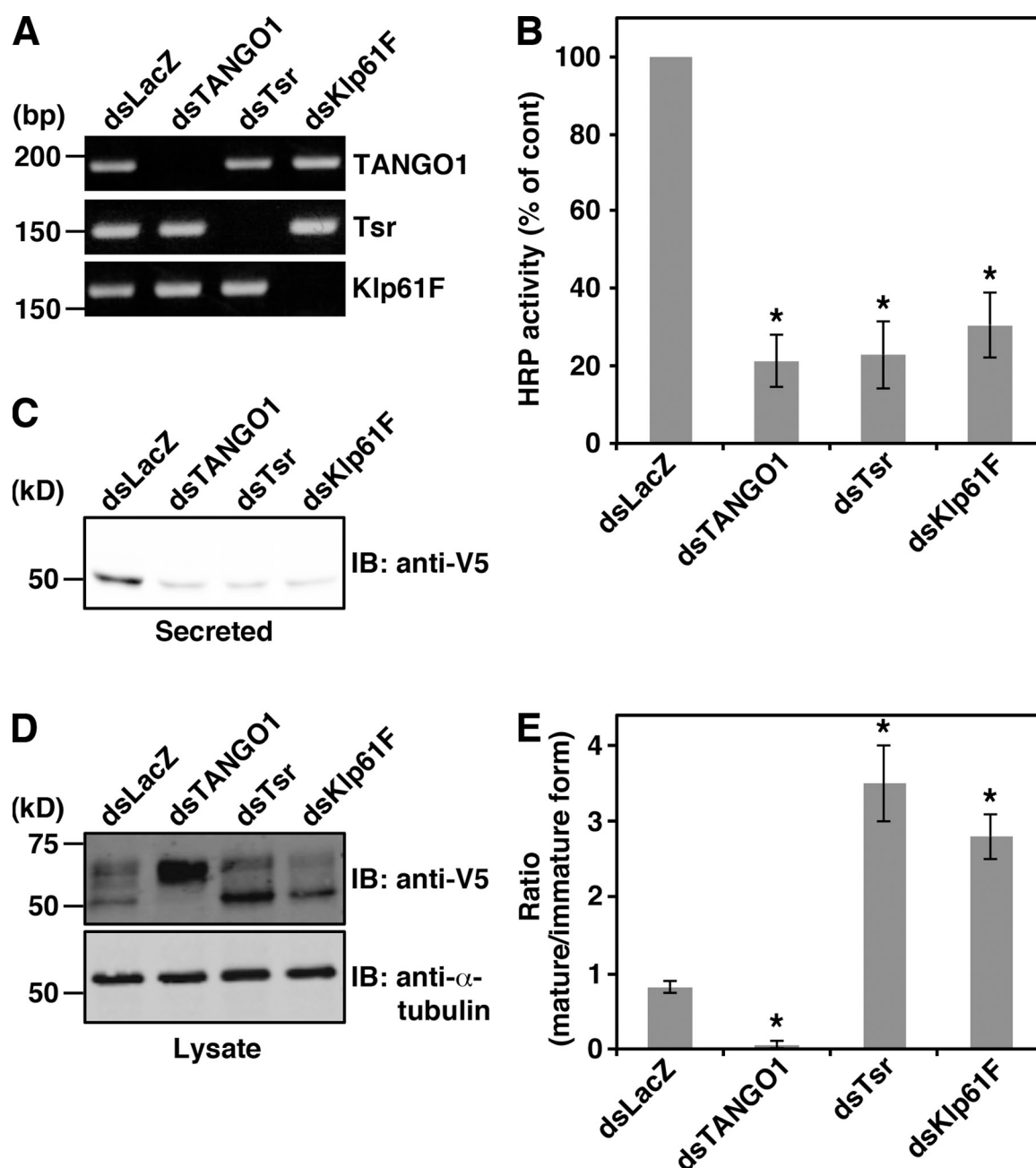
Figure 1. **Klp61F knockdown inhibits post-Golgi transport in _Drosophila_ S2 cells.** _Drosophila_ S2 cells transformed to stably express ssHRP-V5 were transfected with dsRNAs for LacZ (dsLacZ: control), TANGO1 (dsTANGO1), twinstar (dsTsr), or Klp61F (dsKlp61F). (A) The knockdown efficiency was monitored by RT-PCR. (B) HRP activity in the medium from control, TANGO1, Tsr, and Klp61F knockdown cells was detected by ECL and normalized to the levels detected in the cell lysates. The average values of three independent experiments are shown (mean ± SD). Stars indicate P < 0.005. (C–E) The amount of secreted (C) and intracellular (D) HRP-V5 was measured by Western blotting the medium and the cell lysate with anti-V5 tag antibody. To monitor the amounts of proteins loaded, α-tubulin in the cell lysate was used as a marker. (E) Ratio of the 50-kD (mature form) to 65-kD (immature form) polypeptides of HRP-V5. The average values of three independent experiments are shown (mean ± SD). Stars indicate P < 0.005.

top row). However, by live-cell imaging, i.e., without fixation, GFP-Eg5 was found both on fibrous structures and in the cytoplasm (Fig. S3 C). In cells that had been permeabilized with digitonin, washed to remove the cytoplasmic proteins, and fixed, we could clearly detect GFP-Eg5 attached to cytoplasmic microtubules and PAUF-containing CARTS were located on the Eg5-positive microtubules (Fig. S3 B, bottom and middle rows, respectively).

Eg5 is required for the migration of CARTS

These findings prompted us to test the role of Eg5 in the migration of CARTS on cytoplasmic microtubules. HEK 293T cells were transfected with a plasmid for PAUF-MycHis alone (control) or in combination with a plasmid for Myc-Eg5 T112N, a mutant of Eg5, which is defective in ATP hydrolysis (Blangy et al., 1998). 5 h after transfection, 2 mM thymidine was added
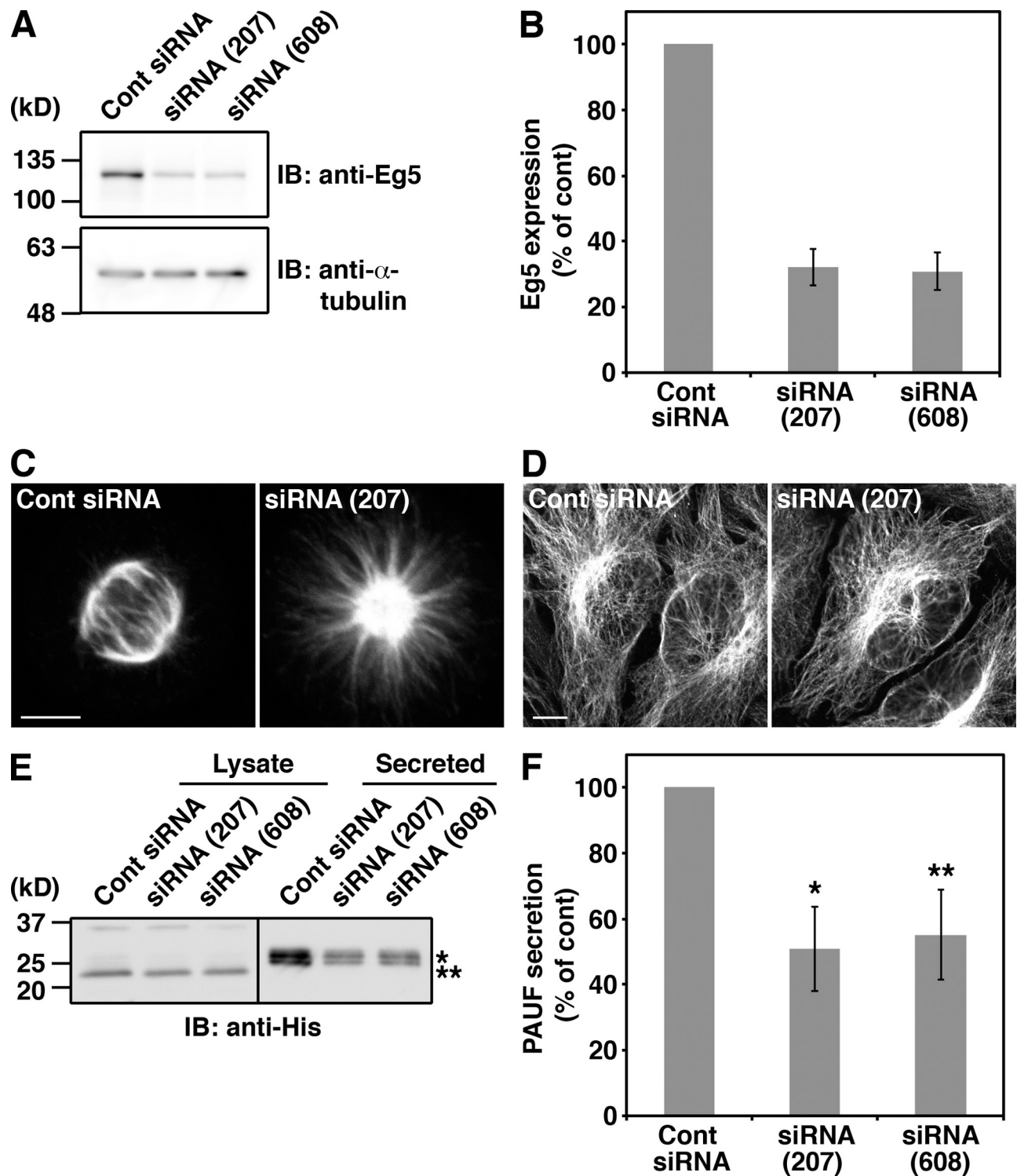
Figure 2. **Eg5 knockdown inhibits PAUF secretion in HeLa cells.** HeLa cells were transfected with control (cont) siRNA or siRNA oligos specific for Eg5. (A and B) 48 h after siRNA transfection, the cell lysates were collected and Western blotted with anti-Eg5 and anti–α-tubulin antibodies, respectively. (B) Quantification of the expression levels of Eg5 upon RNAi. The average values of four independent experiments are shown (mean ± SD). (C) 48 h after siRNA transfection, the cells were fixed and visualized with anti–α-tubulin antibody. Bar, 5 μm. (D) 24 h after siRNA transfection, 2 mM thymidine was added to the medium, and 24 h later the cells were fixed and visualized with anti–α-tubulin antibody. Bar, 10 μm. (E and F) 20 h after siRNA transfection, the cells were transfected with a plasmid for PAUF-MycHis and 4 h later 2 mM thymidine was added to the medium. The medium and the cell lysate were Western blotted with anti-His antibody. Single and double star denote the mature and immature form of PAUF, respectively. (F) Quantification of PAUF secretion. The amount of secreted PAUF was normalized with the expression levels. The average values of four independent experiments are shown (mean ± SD). Single and double star indicate $P < 0.01$ and $P < 0.05$, respectively.
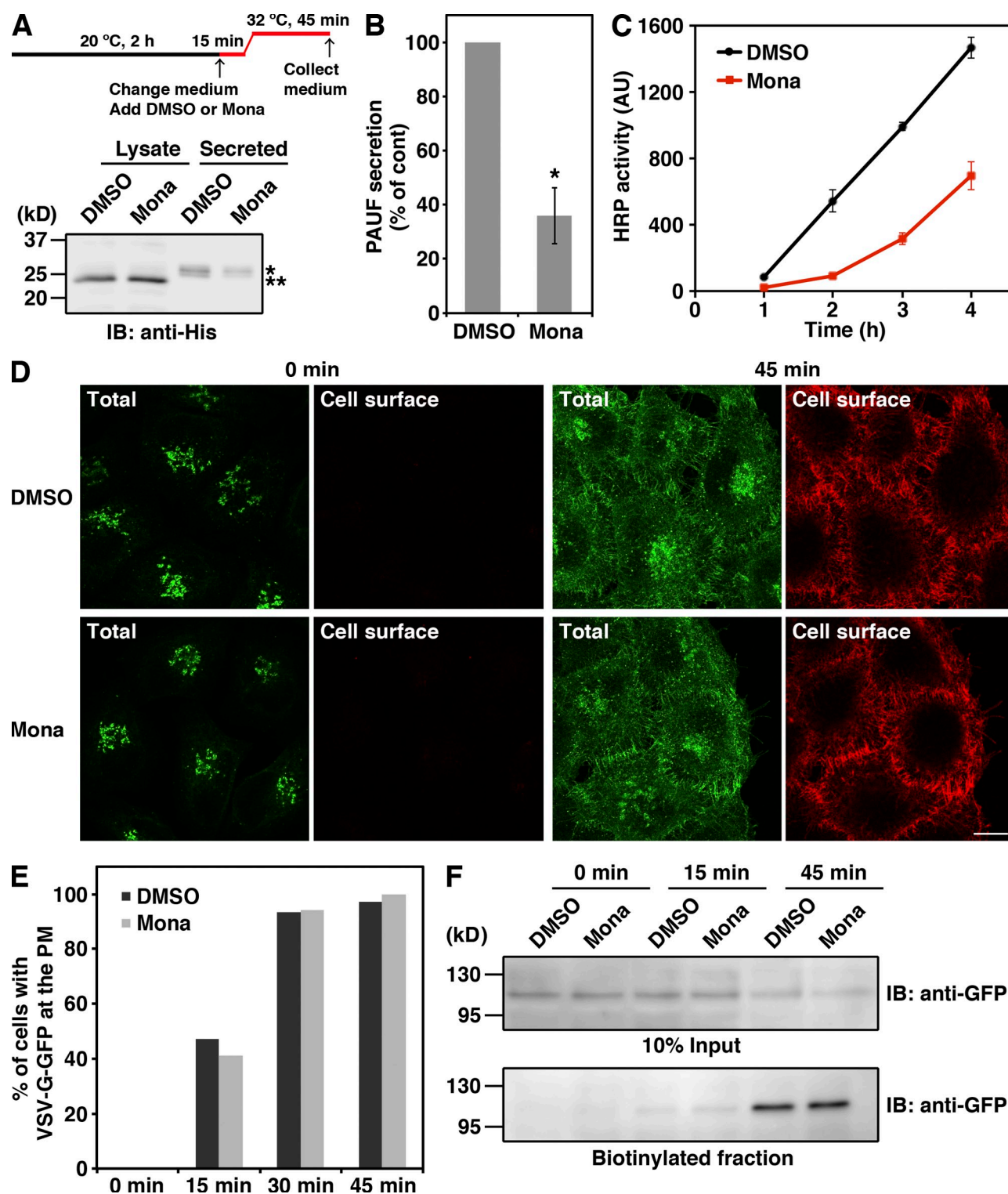
Figure 3.   **Monastrol treatment inhibits PAUF and HRP secretion.** (A and B) Secretion of PAUF-MycHis by HeLa cells treated with DMSO (control) or 100 µM monastrol (Mona) was monitored by Western blotting the cell lysate and the medium with anti-His antibody. Single and double star denote the mature and immature form of PAUF, respectively. (B) Quantification of PAUF secretion. The amount of secreted PAUF was normalized to the total cellular levels. The average values of three independent experiments are shown (mean ± SD). Star indicates $P < 0.005$. (C) HeLa-ssHRP cells were incubated at 37°C with medium containing DMSO or 100 µM monastrol. At the indicated times, the medium was tested for HRP activity by using ECL. Values were corrected for a 21.3% loss of enzymatic activity of HRP by monastrol. (D–F) HeLa-VSV-G-GFP cells were incubated at 20°C for 105 min in the presence of 100 µM cycloheximide, after which the incubation was continued in the presence of DMSO or 100 µM monastrol for 15 min. The cells were then shifted to 32°C for the indicated time. (D) The cells were fixed and incubated with anti–VSV-G antibody without cell permeabilization to specifically detect the cell surface VSV-G-GFP (red) in the total protein (green). Bar, 10 µm. (E) Quantification of the VSV-G trafficking to the cell surface. The percentage of DMSO and monastrol-treated cells with VSV-G-GFP at the plasma membrane (PM) at the indicated time points is shown. The data shown are from a single representative experiment out of two repeats. For the experiment shown, $n = 103$–124 cells per condition. (F) VSV-G-GFP at the cell surface was monitored by a cell surface biotinylation assay as described in Materials and methods.
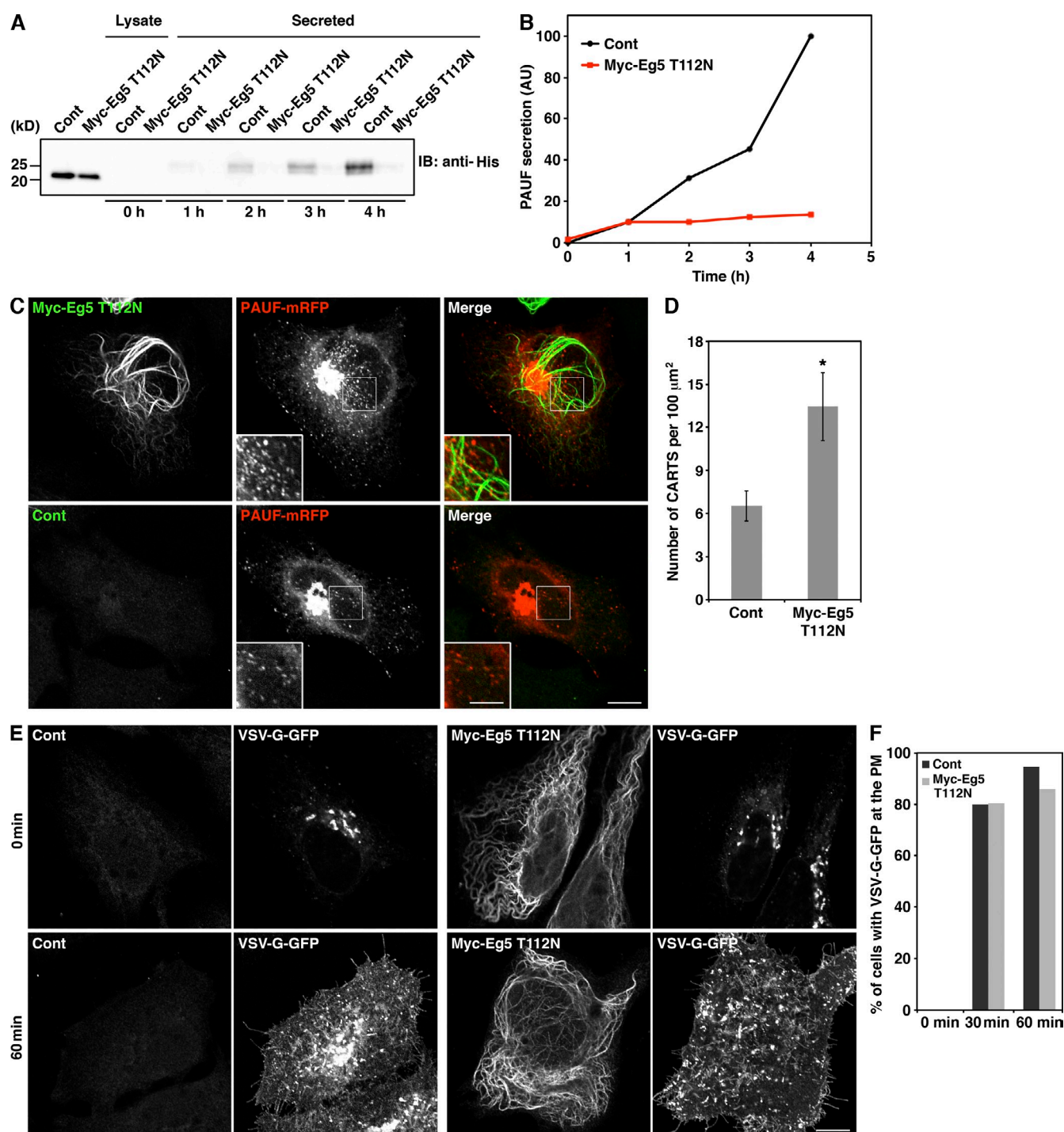
Figure 4. **Eg5 T112N expression inhibits PAUF secretion and causes accumulation of CARTS.** (A and B) HEK 293T cells were transfected with a plasmid for PAUF-MycHis (control) or plasmids for Myc-Eg5 T112N and PAUF-MycHis. 5 h after transfection, 2 mM thymidine was added to the medium, and 18 h later the cells were washed and incubated with fresh medium. At the indicated time points, the medium was Western blotted with anti-His antibody. (B) Quantification of PAUF secretion. The amount of secreted PAUF was normalized with the total cellular levels. The data shown are from a single representative experiment out of three repeats. (C and D) HeLa cells were cotransfected with plasmids for Myc-Eg5 T112N and PAUF-mRFP and visualized by fluorescence microscopy. The cells expressing PAUF-mRFP alone were observed as a control. Bars, 10 µm (inset, 5 µm). (D) Quantification of PAUF containing CARTS. The number of CARTS in control cells (n = 1,946 punctate elements in 20 cells) and Myc-Eg5 T112N–expressing cells (n = 3,701 punctate elements in 20 cells) was determined. The average number of CARTS per 100 µm^2 is shown (mean ± SD). Star indicates P < 0.001. (E and F) HeLa cells were cotransfected with plasmids for Myc-Eg5 T112N and VSV-G-GFP. The cells were incubated at 20°C for 2 h in the presence of 20 µg/ml cycloheximide, shifted to 32°C, and fixed at the indicated time points. The cells expressing VSV-G-GFP alone were observed as a control. Bar, 10 µm. (F) Quantification of the VSV-G trafficking to the cell surface. The percentage of control and Myc-Eg5 T112N–expressing cells with VSV-G-GFP at the plasma membrane (PM) at the indicated time points is shown. The data shown are from a single representative experiment out of two repeats. For the experiment shown, n = 55–58 cells per condition.

to the medium, and 18 h later cells were washed and incubated with fresh medium. At the indicated times, the medium was collected and analyzed by Western blotting with anti-His antibody. Our data reveal that Eg5 T112N expression inhibited the secretion of PAUF (Fig. 4, A and B).

We then tested the effect of Eg5 T112N expression on the distribution of CARTS in HeLa cells. HeLa cells were cotransfected with plasmids for Myc-Eg5 T112N and PAUF-mRFP. After 20 h, the cells were fixed and visualized with anti-Myc antibody. As reported before (Blangy et al., 1998), expression of Eg5 T112N caused microtubule bundling (Fig. 4 C, top-left panel). In Myc-Eg5 T112N expressing cells, PAUF containing CARTS were accumulated around the pericentriolar Golgi complex and there was a twofold increase in the average number of CARTS compared with control cells (Fig. 4, C and D). To test the effect of Eg5 T112N on VSV-G transport, HeLa cells were cotransfected with plasmids for Myc-Eg5 T112N and VSV-G-GFP. After incubation at 40°C for 16 h to synchronize export of VSV-G from the ER, the cells were incubated at 20°C for 2 h in the presence of cycloheximide, and then shifted to 32°C for 30 and 60 min to release VSV-G-GFP from the TGN. There was no significant delay in the transport of VSV-G-GFP to the plasma membrane in cells expressing Myc-Eg5 T112N (Fig. 4, E and F).

Does expression of Eg5 T112N affect the kinetics of CARTS migration in HeLa cells? The migration of PAUF-mRFP–containing CARTS was examined by live-cell imaging and most of them were found to be static or move a short distance on microtubules (Videos 2–4 and Fig. 5 A). In GFP-Eg5 T112N–expressing cells the slow migrating pool of CARTS was increased compared with control cells expressing PAUF-mRFP alone (Fig. 5 B).

Eg5 is not required for the biogenesis of CARTS

Our data suggests that Eg5 is not required for the biogenesis of CARTS but for their migration to the cell surface. To formally test this proposal, we used an assay that reconstitutes the biogenesis of CARTS (Wakana et al., 2012). Permeabilized HeLa cells were pretreated with monastrol to inhibit Eg5 at 32°C for 10 min and then incubated in the presence of rat liver cytosol and an ATP regenerating system at 32°C for 45 min. CARTS were then collected by high-speed centrifugation and Western blotted with anti-TGN46 antibody as described previously (Wakana et al., 2012). Monastrol treatment did not inhibit the production of CARTS (Fig. 5, C and D). Treatment of the reaction mixture with nocodazole, to depolymerize microtubules, also did not affect the production of CARTS (Fig. 5, C and D).

Altogether, our findings reveal that Eg5 is required for the migration of CARTS in nonmitotic cells. Eg5 is a plus end–directed bipolar kinesin, which cross-links and slides antiparallel microtubules during bipolar spindle assembly (Sharp et al., 1999; Kapoor and Mitchison, 2001; Kwok et al., 2004; Miyamoto et al., 2004; Kapitein et al., 2005; Valentine et al., 2006; Brust-Mascher et al., 2009). It is plausible that CARTS are loaded onto anti-parallel microtubules emanating from the TGN, which slide against each other through the action of Eg5, thus propelling CARTS from the TGN toward the cell periphery.

This process might also involve another kinesin but CARTS also contain myosin II (Wakana et al., 2012), which likely promotes their migration through the cortical actin for fusion with the plasma membrane.

Materials and methods

Antibodies and reagents
Monoclonal antibodies against α-tubulin and β-actin were purchased from Sigma-Aldrich. Monoclonal antibodies against V5 tag, His, and Myc were purchased from Invitrogen, QIAGEN, and Santa Cruz Biotechnology, Inc., respectively. Polyclonal antibodies against α-tubulin, GFP, and TGN46 were purchased from Abcam, Santa Cruz Biotechnology, Inc., and AbD Serotec, respectively. Mouse monoclonal anti–VSV-G antibody (clone 8G5F11) was described previously (Lefrancois and Lyles, 1982) and donated by D.S. Lyles (Wake Forest University School of Medicine, Winston-Salem, NC). Rabbit polyclonal antibodies against Eg5, KIF15, and KIF22 were gifts from I. Vernos (Centre for Genomic Regulation, Barcelona, Spain). Monastrol and nocodazole were purchased from Sigma-Aldrich. The plasmids encoding PAUF-MycHis, GFP-Eg5, and Myc-Eg5 were gifts from S.S. Koh (Korea Research Institute of Bioscience and Biotechnology, Daejeon, Korea), T.U. Mayer (University of Konstanz, Konstanz, Germany), and J. Roig (Institute for Research in Biomedicine, Barcelona, Spain), respectively. The sources of other plasmids are described previously (Wakana et al., 2012).

Cell culture and transfection
Drosophila S2 cells transformed to stably express ssHRP-V5 on a Cu^{2+}-inducible promoter (Bard et al., 2006) were grown in Schneider's medium (Invitrogen) supplemented with 10% fetal calf serum, 100 U/ml penicillin, and 100 µg/ml streptomycin at 20°C. HeLa cells stably expressing ssHRP or VSV-G-GFP (gifts from I. Stamenkovic, University of Lausanne, Lausanne, Switzerland), HeLa, and HEK 293T cells were grown in DMEM supplemented with 10% fetal calf serum. Plasmid and siRNA transfection were performed using X-tremeGENE 9 DNA transfection reagent (Roche) and Oligofectamine reagent (Invitrogen), respectively, according to the manufacturer's protocol.

### HRP secretion assay in *Drosophila* S2 cells
DsRNA oligos specific for TANGO1, twinstar, and Klp61F were purchased from the *Drosophila* RNAi Screening Center (Boston, MA). For transfection of *Drosophila* S2 cells with dsRNA, cells were seeded in a 96-well plate with 1 µg of dsRNA in triplicate in 60 µl of medium without serum. After 2 h, serum was added to the medium and after 5 d ssHRP-V5 expression was induced by replacing culture medium with 100 µl of medium containing 0.5 mM $CuSO_4$. 12 h later, the medium and the cell lysates were harvested for HRP secretion assay. Cells were lysed in 100 µl of lysis buffer (50 mM Tris, pH 7.4, 150 mM NaCl, 0.1% sodium dodecyl sulfate [SDS], 1% Nonidet P-40 [NP-40], and 0.5% sodium deoxycholate) supplemented with protease inhibitors, 1 mM Na_3VO_4, and 25 mM sodium fluoride, centrifuged at 20,000 g for 15 min, and the supernatants were collected. HRP-V5 was detected by measuring chemiluminescence and by Western blotting the medium and the cell lysate. For the chemiluminescence assay, 10 µl of medium was mixed with ECL reagent (Thermo Fisher Scientific) and the luminescence measured with a Victor 3 plate reader (PerkinElmer). Internal HRP activity was measured in 10 µl of the cell lysate for normalization. For the detection by Western blotting, 10 µl of the medium and the cell lysate, respectively, were Western blotted with primary antibodies (anti-V5 tag and anti–α-tubulin antibodies) and secondary antibodies conjugated to DyLight 800 and Alexa Fluor 680. The fluorescent bands were visualized using the Odyssey Infrared Imaging System (LI-COR Biosciences).

HRP secretion assay in HeLa cells
HeLa-ssHRP cells were washed with medium and incubated at 37°C with 1 ml medium containing 100 µM monastrol or DMSO in a 12-well plate. Alternatively, HeLa-ssHRP cells were transfected with control siRNA, Eg5-, KIF15-, or KIF22-specific siRNA oligos. 24 h later, 2 mM thymidine was added to the medium to inhibit the entry of cells into mitosis, and after 24 h incubation the cells were washed with medium and incubated with 1 ml of complete medium in a 12-well plate. At the indicated times, 50 µl of the medium was collected, mixed with ECL reagent, and the chemiluminescence measured in a Victor 3 plate reader. For normalization, cells were lysed with lysis buffer supplemented with protease inhibitors to quantitate intracellular HRP activity.

Figure 5. Eg5 is required for migration of CARTS. (A and B) HeLa cells cotransfected with plasmids for GFP-Eg5 T112N and PAUF-mRFP were imaged at 1-s interval for ~3 min. The cells expressing PAUF-mRFP alone were observed as a control. (A) Tracking of CARTS was performed using Imaris software. The tracks are colorized as shown in the time scale at the bottom. The images of the indicated time points are shown. Bars, 5 µm. See also Videos 2–4. (B) Histogram of velocity distribution of CARTS migration in control cells ($n = 546$ punctate elements in 7 cells) and GFP-Eg5 T112N–expressing cells ($n = 829$ punctate elements in 7 cells). The migration rate is shown according to the speed mean values. A χ^2 test shows that both speed distributions are significantly different ($\chi^2 = 129.8$; $P < 0.001$). (C and D) The reaction mixture for the biogenesis of CARTS was incubated with DMSO (control), 100 µM monastrol (Mona), or 20 µM nocodazole (Noc) at 4 or 32°C. The high-speed pellet containing CARTS was Western blotted with anti-TGN46 antibody. The input refers to permeabilized HeLa cells used as starting material in these experiments. (D) Quantification of CARTS formation. The average values of three independent experiments are shown (mean ± SD).
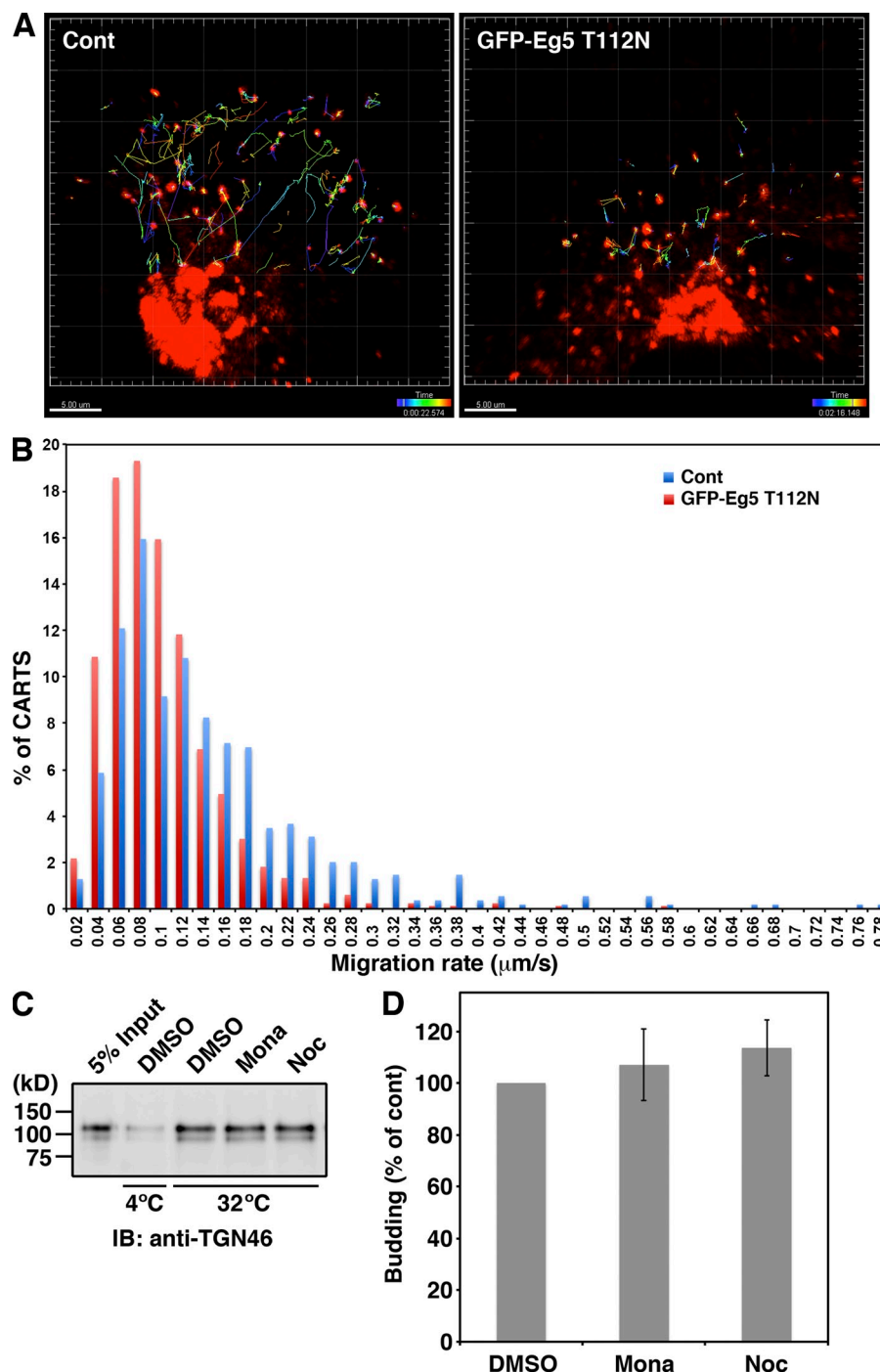
RT-PCR

RNA was prepared using the RNAeasy Mini kit (QIAGEN) and cDNAs were synthesized with the Cloned AMV First-Strand cDNA Synthesis kit (Invitrogen) according to the manufacturer's protocol. TANGO1, twinstar, and Klp61F cDNA were amplified by PCR with specific primers.

RNA interference in HeLa cells

The sequence of control siRNA oligo is 5′-CCACUUUAACUUAGACUAC-GCAAUU-3′. The sequences of siRNA oligos targeting human Eg5 are 5′-UAUGGUGUUUGGAGCAUCUACUAAA-3′(207) and 5′-CAGUACA-CAACAAGGAUGAAGUCUA-3′ (608). The sequences of siRNA oligos targeting human KIF15 and KIF22 are 5′-GGACAUAAAUUGCAAAUAC-3′ and 5′-GCUCUCUAGAGAUUGCUAA-3′, respectively.

Immunofluorescence microscopy

Cells were fixed with 4% paraformaldehyde in phosphate-buffered saline (PBS) at room temperature for 20 min, permeabilized with 0.2% Triton X-100 for 30 min, and then blocked with 2% bovine serum albumin (BSA) for 30 min. The cells were labeled with the indicated primary antibodies and secondary antibodies conjugated to Alexa Fluor 488 and 594. The samples were analyzed with a confocal microscope (SPE or SP5 II; Leica) with the 63× ACS Apo NA 1.3 objective and LASAF software. Image processing and quantification of CARTS were performed with ImageJ software (National Institutes of Health). The fluorescence signal of PAUF-mRFP containing punctae was distinguished from the background by setting a threshold and analyzed at a set size within 0.05–2.00 µm².

PAUF secretion assay

HeLa cells were transfected with control siRNA or siRNA oligos targeting Eg5. 20 h after siRNA transfection, cells were transfected with a plasmid for PAUF-MychHis, and 4 h later 2 mM thymidine was added to the medium to inhibit mitotic entry. 20 h later, the medium was replaced with Opti-MEM and the cells were incubated at 20°C for 2 h and then shifted to 32°C for 1 h to restore cargo export from the TGN. For experiments with

monastrol, PAUF-MycHis–expressing cells were incubated in Opti-MEM at 20°C for 2 h, pretreated with DMSO (control) or 100 µM monastrol for 15 min, and then shifted to 32°C for 45 min. Secreted proteins in the medium were precipitated with trichloroacetic acid; the precipitates and cell lysates were Western blotted with anti-His antibody.

Cell surface biotinylation assay

HeLa-VSV-G-GFP cells were cultured at 40°C for 48 h. The cells were then incubated at 20°C for 105 min in the presence of 100 µM cycloheximide, after which the incubation was continued in the presence of DMSO or 100 µM monastrol for 15 min. The cells were shifted to 32°C for various time points, after which the cells were washed three times with ice-cold PBS+ (PBS with 0.1 mM $CaCl_2$ and 0.1 mM $MgCl_2$). The cells were biotinylated with 1 mg/ml sulfo-NHS-LC-Biotin (Thermo Fisher Scientific) in PBS+ for 30 min on ice. The cells were washed twice with PBS+ and biotin was quenched by incubation with 100 mM glycine and 0.3% BSA in PBS+ for 30 min on ice. After washing twice with PBS+, the cells were lysed with PBS containing 2% NP-40, 0.2% SDS, and protease inhibitors for 10 min on ice. The lysates were centrifuged at 16,000 g for 15 min and the resulting supernatants were incubated with equilibrated Neutravidin Agarose resin (Thermo Fisher Scientific) overnight at 4°C while rotating. The resins were washed twice with PBS containing 2% NP-40 and 0.2% SDS and twice with PBS. The resins were eluted with SDS sample buffer. VSV-G-GFP was detected using an anti-GFP antibody.

Live-cell imaging

HeLa cells were cotransfected with plasmids for PAUF-mRFP and GFP–α-tubulin or GFP-Eg5 T112N. 20 h later, medium was replaced with phenol red–free Opti-MEM and cells were maintained in 5% CO_2 at 37°C during live-cell imaging. Images were acquired continuously with time intervals between frames of 1 s for ∼3 min by use of a confocal microscope (Fluoview FV1000; Olympus) with a UPLSAPO 60x O NA 1.35 objective and FV10-ASW software. The images were processed with ImageJ software. Single CARTS were identified and tracked using Imaris 7.6 software (Bitplane AG). The estimated diameter for structures to be tracked was set to 0.7 µm. Autoregressive motion was selected as the tracking algorithm. The parameters "MaxDistance" and "MaxGapSize" of the software were set to 1 and 3, respectively. All tracks with duration shorter than 5 s were discarded from the quantification.

Plasmid construction

A point mutation (T112N) in human Eg5 was introduced into plasmids for Myc-Eg5 and GFP-Eg5 (gifts from J. Roig and T.U. Mayer, respectively) by PCR using primers designed for replacing threonine 112 with asparagine in the expressed protein.

CARTS biogenesis

As described previously (Wakana et al., 2012), HeLa cells suspended in buffer A (20 mM Hepes, pH 7.4, 250 mM D-sorbitol, and 150 mM potassium acetate) were permeabilized with 40 µg/ml digitonin for 5 min on ice and then washed with buffer A supplemented with 1 M potassium chloride. The permeabilized HeLa cells were pretreated with DMSO (control), monastrol, or nocodazole at 32°C for 10 min and then incubated at 32°C for 45 min in buffer A supplemented with an ATP regenerating system (1 mM ATP, 40 mM creatine phosphate, and 0.2 mg/ml creatine kinase) and 0.5 mg/ml rat liver cytosol. Transport carriers were separated from the permeabilized cells by centrifugation at 10,000 g (low speed) for 10 min, and the supernatant was centrifuged at 100,000 g (high speed) for 1 h. The pellet was solubilized with SDS sample buffer and Western blotted with anti-TGN46 antibody to estimate the amount of generated CARTS.

Online supplemental material

Fig. S1 shows the organization of cytoplasmic microtubules and the Golgi complex upon Eg5 knockdown or inactivation in nonmitotic cells. Fig. S2 shows the kinetics of HRP secretion in control cells and Eg5, KIF15, and KIF22 knockdown cells. Fig. S3 shows distribution of CARTS along cytoplasmic microtubules and colocalization of GFP-Eg5 with cytoplasmic microtubules in nonmitotic cells. Video 1 shows the kinetics of CARTS trafficking along microtubules. Videos 2 and 3 show the kinetics of CARTS in a control cell and a cell expressing GFP-Eg5 T112N, respectively. Video 4 is dual-color live imaging of the cell in Video 3. Online supplemental material is available at http://www.jcb.org/cgi/content/full/jcb.201303163/DC1. Additional data are available in the JCB DataViewer at http://dx.doi.org/10.1083/jcb.201303163.dv.

References

Anitei, M., and B. Hoflack. 2011. Exit from the trans-Golgi network: from molecules to mechanisms. *Curr. Opin. Cell Biol.* 23:443–451. http://dx.doi.org/10.1016/j.ceb.2011.03.013

Astanina, K., and R. Jacob. 2010. KIF5C, a kinesin motor involved in apical trafficking of MDCK cells. *Cell. Mol. Life Sci.* 67:1331–1342. http://dx.doi.org/10.1007/s00018-009-0253-6

Bard, F., L. Casano, A. Mallabiabarrena, E. Wallace, K. Saito, H. Kitayama, G. Guizzunti, Y. Hu, F. Wendler, R. Dasgupta, et al. 2006. Functional genomics reveals genes involved in protein secretion and Golgi organization. *Nature.* 439:604–607. http://dx.doi.org/10.1038/nature04377

Blangy, A., H.A. Lane, P. d'Hérin, M. Harper, M. Kress, and E.A. Nigg. 1995. Phosphorylation by p34cdc2 regulates spindle association of human Eg5, a kinesin-related motor essential for bipolar spindle formation in vivo. *Cell.* 83:1159–1169. http://dx.doi.org/10.1016/0092-8674(95)90142-6

Blangy, A., P. Chaussepied, and E.A. Nigg. 1998. Rigor-type mutation in the kinesin-related protein HsEg5 changes its subcellular localization and induces microtubule bundling. *Cell Motil. Cytoskeleton.* 40:174–182. http://dx.doi.org/10.1002/(SICI)1097-0169(1998)40:2<174::AID-CM6>3.0.CO;2-F

Brust-Mascher, I., P. Sommi, D.K. Cheerambathur, and J.M. Scholey. 2009. Kinesin-5-dependent poleward flux and spindle length control in *Drosophila* embryo mitosis. *Mol. Biol. Cell.* 20:1749–1762. http://dx.doi.org/10.1091/mbc.E08-10-1033

Burgo, A., V. Proux-Gillardeaux, E. Sotirakis, P. Bun, A. Casano, A. Verraes, R.K. Liem, E. Formstecher, M. Coppey-Moisan, and T. Galli. 2012. A molecular network for the transport of the TI-VAMP/VAMP7 vesicles from cell center to periphery. *Dev. Cell.* 23:166–180. http://dx.doi.org/10.1016/j.devcel.2012.04.019

Cole, D.G., W.M. Saxton, K.B. Sheehan, and J.M. Scholey. 1994. A "slow" homotetrameric kinesin-related motor protein purified from *Drosophila* embryos. *J. Biol. Chem.* 269:22913–22916.

Cottingham, F.R., L. Gheber, D.L. Miller, and M.A. Hoyt. 1999. Novel roles for *Saccharomyces cerevisiae* mitotic spindle motors. *J. Cell Biol.* 147:335–350. http://dx.doi.org/10.1083/jcb.147.2.335

Grigoriev, I., D. Splinter, N. Keijzer, P.S. Wulf, J. Demmers, T. Ohtsuka, M. Modesti, I.V. Maly, F. Grosveld, C.C. Hoogenraad, and A. Akhmanova. 2007. Rab6 regulates transport and targeting of exocytotic carriers. *Dev. Cell.* 13:305–314. http://dx.doi.org/10.1016/j.devcel.2007.06.010

Hagan, I., and M. Yanagida. 1992. Kinesin-related cut7 protein associates with mitotic and meiotic spindles in fission yeast. *Nature.* 356:74–76. http://dx.doi.org/10.1038/356074a0

Heck, M.M., A. Pereira, P. Pesavento, Y. Yannoni, A.C. Spradling, and L.S. Goldstein. 1993. The kinesin-like protein KLP61F is essential for mitosis in *Drosophila*. *J. Cell Biol.* 123:665–679. http://dx.doi.org/10.1083/jcb.123.3.665

Hirokawa, N., and Y. Noda. 2008. Intracellular transport and kinesin superfamily proteins, KIFs: structure, function, and dynamics. *Physiol. Rev.* 88:1089–1118. http://dx.doi.org/10.1152/physrev.00023.2007

Jaulin, F., X. Xue, E. Rodriguez-Boulan, and G. Kreitzer. 2007. Polarization-dependent selective transport to the apical membrane by KIF5B in MDCK cells. *Dev. Cell.* 13:511–522. http://dx.doi.org/10.1016/j.devcel.2007.08.001

Kapitein, L.C., E.J. Peterman, B.H. Kwok, J.H. Kim, T.M. Kapoor, and C.F. Schmidt. 2005. The bipolar mitotic kinesin Eg5 moves on both microtubules that it crosslinks. *Nature.* 435:114–118. http://dx.doi.org/10.1038/nature03503

Kapoor, T.M., and T.J. Mitchison. 2001. Eg5 is static in bipolar spindles relative to tubulin: evidence for a static spindle matrix. *J. Cell Biol.* 154:1125–1133. http://dx.doi.org/10.1083/jcb.200106011

Kwok, B.H., J.G. Yang, and T.M. Kapoor. 2004. The rate of bipolar spindle assembly depends on the microtubule-gliding velocity of the mitotic kinesin Eg5. *Curr. Biol.* 14:1783–1788. http://dx.doi.org/10.1016/j.cub.2004.09.052

Lawrence, C.J., R.K. Dawe, K.R. Christie, D.W. Cleveland, S.C. Dawson, S.A. Endow, L.S. Goldstein, H.V. Goodson, N. Hirokawa, J. Howard, et al. 2004.

A standardized kinesin nomenclature. *J. Cell Biol.* 167:19–22. http://dx.doi.org/10.1083/jcb.200408113

Le Guellec, R., J. Paris, A. Couturier, C. Roghi, and M. Philippe. 1991. Cloning by differential screening of a Xenopus cDNA that encodes a kinesin-related protein. *Mol. Cell. Biol.* 11:3395–3398.

Lefrancois, L., and D.S. Lyles. 1982. The interaction of antibody with the major surface glycoprotein of vesicular stomatitis virus. I. Analysis of neutralizing epitopes with monoclonal antibodies. *Virology.* 121:157–167. http://dx.doi.org/10.1016/0042-6822(82)90125-8

Mayer, T.U., T.M. Kapoor, S.J. Haggarty, R.W. King, S.L. Schreiber, and T.J. Mitchison. 1999. Small molecule inhibitor of mitotic spindle bipolarity identified in a phenotype-based screen. *Science.* 286:971–974. http://dx.doi.org/10.1126/science.286.5441.971

Mellman, I., and W.J. Nelson. 2008. Coordinated protein sorting, targeting and distribution in polarized cells. *Nat. Rev. Mol. Cell Biol.* 9:833–845. http://dx.doi.org/10.1038/nrm2525

Miyamoto, D.T., Z.E. Perlman, K.S. Burbank, A.C. Groen, and T.J. Mitchison. 2004. The kinesin Eg5 drives poleward microtubule flux in Xenopus laevis egg extract spindles. *J. Cell Biol.* 167:813–818. http://dx.doi.org/10.1083/jcb.200407126

Nakagawa, T., M. Setou, D. Seog, K. Ogasawara, N. Dohmae, K. Takio, and N. Hirokawa. 2000. A novel motor, KIF13A, transports mannose-6-phosphate receptor to plasma membrane through direct interaction with AP-1 complex. *Cell.* 103:569–581. http://dx.doi.org/10.1016/S0092-8674(00)00161-6

Noda, Y., Y. Okada, N. Saito, M. Setou, Y. Xu, Z. Zhang, and N. Hirokawa. 2001. KIFC3, a microtubule minus end-directed motor for the apical transport of annexin XIIIb-associated Triton-insoluble membranes. *J. Cell Biol.* 155:77–88. http://dx.doi.org/10.1083/jcb.200108042

Saito, K., M. Chen, F. Bard, S. Chen, H. Zhou, D. Woodley, R. Polischuk, R. Schekman, and V. Malhotra. 2009. TANGO1 facilitates cargo loading at endoplasmic reticulum exit sites. *Cell.* 136:891–902. http://dx.doi.org/10.1016/j.cell.2008.12.025

Saunders, W.S., and M.A. Hoyt. 1992. Kinesin-related proteins required for structural integrity of the mitotic spindle. *Cell.* 70:451–458. http://dx.doi.org/10.1016/0092-8674(92)90169-D

Sawin, K.E., K. LeGuellec, M. Philippe, and T.J. Mitchison. 1992. Mitotic spindle organization by a plus-end-directed microtubule motor. *Nature.* 359:540–543. http://dx.doi.org/10.1038/359540a0

Sharp, D.J., K.L. McDonald, H.M. Brown, H.J. Matthies, C. Walczak, R.D. Vale, T.J. Mitchison, and J.M. Scholey. 1999. The bipolar kinesin, KLP61F, cross-links microtubules within interpolar microtubule bundles of *Drosophila* embryonic mitotic spindles. *J. Cell Biol.* 144:125–138. http://dx.doi.org/10.1083/jcb.144.1.125

Vale, R.D. 2003. The molecular motor toolbox for intracellular transport. *Cell.* 112:467–480. http://dx.doi.org/10.1016/S0092-8674(03)00111-9

Valentine, M.T., P.M. Fordyce, and S.M. Block. 2006. Eg5 steps it up! *Cell Div.* 1:31. http://dx.doi.org/10.1186/1747-1028-1-31

von Blume, J., J.M. Duran, E. Forlanelli, A.M. Alleaume, M. Egorov, R. Polishchuk, H. Molina, and V. Malhotra. 2009. Actin remodeling by ADF/cofilin is required for cargo sorting at the trans-Golgi network. *J. Cell Biol.* 187:1055–1069. http://dx.doi.org/10.1083/jcb.200908040

Wakana, Y., J. van Galen, F. Meissner, M. Scarpa, R.S. Polishchuk, M. Mann, and V. Malhotra. 2012. A new class of carriers that transport selective cargo from the trans Golgi network to the cell surface. *EMBO J.* 31:3976–3990. http://dx.doi.org/10.1038/emboj.2012.235

Zanetti, G., K.B. Pahuja, S. Studer, S. Shim, and R. Schekman. 2012. COPII and the regulation of protein sorting in mammals. *Nat. Cell Biol.* 14:20–28. http://dx.doi.org/10.1038/ncb2390